



Abnormalities of cingulate gyrus neuroanatomy in schizophrenia

Lei Wang^{a,*}, Malini Hosakere^f, Joshua C.L. Trein^a, Alex Miller^a,
J. Tilak Ratnanather^{f,g}, Deanna M. Barch^b, Paul A. Thompson^c, Anqi Qiu^f,
Mokhtar H. Gado^d, Michael I. Miller^{f,g}, John G. Csernansky^{a,e}

^a Department of Psychiatry, Washington University School of Medicine, Box 8134, 660 S. Euclid Ave., St. Louis MO 63110, United States

^b Department of Psychology, Washington University School of Medicine, St. Louis MO, United States

^c Division of Biostatistics, Washington University School of Medicine, St. Louis MO, United States

^d Department of Radiology, Washington University School of Medicine, St. Louis MO, United States

^e Department of Anatomy and Neurobiology, Washington University School of Medicine, St. Louis MO, United States

^f Center for Imaging Science, The Johns Hopkins, University, Baltimore MD, United States

^g Institute for Computational Medicine, The Johns Hopkins, University, Baltimore MD, United States

Received 27 September 2006; received in revised form 17 February 2007; accepted 20 February 2007

Abstract

Objective and methods: Abnormalities of the neuroanatomy of the gray matter of the cingulate gyrus, especially its anterior segment, have been suggested to be an important characteristic of schizophrenia. In this study, T1-weighted magnetic resonance scans were collected in 53 individuals with schizophrenia and 68 comparison subjects matched for age, gender, race and parental socioeconomic status. We applied Labeled Cortical Mantle Distance Mapping to assess the volume, surface area and thickness of the cortical mantle within the anterior (AC) and posterior (PC) segments of the cingulate gyrus, excluding the paracingulate gyrus, and related these anatomical measures to measures of psychopathology and illness duration.

Results: After covarying for total cerebral volume, individuals with schizophrenia showed smaller AC gray matter volume ($p=0.024$), thickness (trend, $p=0.081$), but not surface area ($p=0.16$), than comparison subjects. Similar group differences were found for PC gray matter volume ($p=0.0005$) and thickness (trend, $p=0.055$), but not surface area ($p=0.15$). Across both groups, there was a significant L > R asymmetry in thickness of the AC, and a significant L > R asymmetry in the surface area of the PC. However, there were no significant group-by-hemisphere interactions. In the individuals with schizophrenia, thinning of the AC, but not the PC, was correlated with a longer duration of illness and a greater severity of psychotic symptoms.

Conclusions: Individuals with schizophrenia showed smaller gray matter volumes across the entire cingulate gyrus, mostly due to a reduction in cortical mantle thickness. However, structural measures of the AC were more closely related to clinical features of the illness.

© 2007 Elsevier B.V. All rights reserved.

Keywords: Depth Map; Thickness; Surface area; Cortex; Thinning

1. Introduction

Post-mortem studies of individuals with schizophrenia have revealed cellular abnormalities in the cingulate gyrus, especially its anterior segment (Benes, 1991;

* Corresponding author. Tel.: +1 314 362 2417.

E-mail address: lei@wustl.edu (L. Wang).

Benes and Bird, 1987; Benes et al., 1991, 2001; Chana et al., 2003; Dolan et al., 1995; Todtenkopf et al., 2005). The results of such studies suggest that reduced density of selected cell types in granular layers (Todtenkopf et al., 2005), reduced neuronal size (Bouras et al., 2001; Chana et al., 2003; Ongur et al., 1998) and reduced glial density (Cotter et al., 2001) are features of the neuropathology of schizophrenia. However, formulations of the pathogenesis of the schizophrenia, especially those that implicate *N*-methyl-D-aspartate (NMDA) receptor hypofunction (Olney and Farber, 1995) predict the presence of pathology across the entire anterior-to-posterior extent of the cingulate gyrus.

Reports from *in vivo* neuroimaging studies of ventricular enlargement in the vicinity of the cingulate gyrus in schizophrenia subjects initially inspired interest in more direct examination of this structure (Andreasen et al., 1990). However, *in vivo* neuroimaging studies of the cingulate gyrus, *per se*, in schizophrenia versus healthy comparison subjects have been inconclusive, with some studies showing evidence of gray matter volume reduction in the cingulate gyrus (Goldstein et al., 2002; Ha et al., 2004; Mitelman et al., 2005; Narr et al., 2005; Sigmundsson et al., 2001), and others showing no group difference (Crespo-Facorro et al., 2000; Hirayasu et al., 1999; Mitelman et al., 2003; Narr et al., 2003; Riffkin et al., 2005; Uematsu and Kaiya, 1989; Young et al., 1991). In addition, the results of these studies have failed to clarify whether structural abnormalities of the cingulate gyrus are confined to the anterior segment or are more generalized (Hulshoff Pol et al., 2001; Mitelman et al., 2005; Sigmundsson et al., 2001). Studies of cingulate gyrus morphology in individuals with schizophrenia have also suggested gender-related volume differences (Goldstein et al., 2002), and the absence of the normative leftward asymmetry (Yucel et al., 2002). Notably, in meta-analyses of *in vivo* neuroimaging studies of individuals with schizophrenia, the cingulate gyrus was not mentioned among the list of cortical/limbic structures known to be affected (Lawrie and Abukmeil, 1998; Wright et al., 2000).

Recently developed methods of computational anatomy can facilitate the characterization of subtle neuroanatomical abnormalities in individuals with neuropsychiatric disorders (Csernansky et al., 2004b). In this study, we employed methods specifically designed and validated for the analysis of the macroscopic features of the neocortical surface; *i.e.*, volume, thickness and surface area (Ratnanather et al., 2004). Because these methods were designed to be applied locally within specific cortical regions, they offer

improved tissue segmentation (Joshi et al., 1999; Miller et al., 2000) as compared to whole-brain methods that are more affected by image inhomogeneities caused by magnetic resonance (MR) field bias (Fischl et al., 2002; Van Leemput et al., 2003).

2. Method

2.1. Participants

Fifty-three individuals with schizophrenia and 68 healthy comparison subjects, matched in age, gender, race, and parental socioeconomic status, gave written informed consent for participation in this study after the risks and benefits of participation were explained to them. Individual demographic and clinical information are summarized in Table 1. The participants in this study were largely overlapping with those described in prior studies of the hippocampus and thalamus (Csernansky et al., 2004a, 2002). Briefly, the diagnosis of each individual was determined by the consensus of a research psychiatrist who conducted a semi-structured interview and a research assistant who used the Structured Clinical Interview for the DSM-IV (SCID-IV) (First et al., 1995) using criteria from the Diagnostic and Statistical Manual for Mental Disorders—Fourth Edition (DSM-IV) (American Psychiatric Association, 1994). No individual had an unstable medical or neurological disorder, a head injury with loss of consciousness, nor did any meet DSM-IV criteria for substance abuse or dependence for 3 months preceding the study. Comparison subjects were also excluded if they had first-degree relatives with a psychotic disorder.

Forty-nine of the 53 individuals with schizophrenia were treated with antipsychotic drugs, and in all individuals with schizophrenia, their symptoms had remained unchanged for at least 2 weeks (Rastogi-Cruz and Csernansky, 1997). The severity of psychopathol-

Table 1
Participants demographic and clinical information

Variables (mean +/- SD [range])	Schizophrenia	Comparison
<i>N</i>	53	68
Age	37.1 (11.9 [20–59])	39.0 (14.4 [20–67])
Gender (male/female)	32/21	35/33
Race (Caucasian/African-American/other)	22/29/2	42/25/1
Parental SES	4.1 (0.90 [2–5])	3.6 (0.97 [1–5])
Age of illness onset	23.1 (8.2 [13–54])	Not applicable
Duration of illness (years)	12.4 (11.9 [0–45])	Not applicable
Total SAPS score	18.6 (17.2 [0–67])	Not applicable
Total SANS score	21.9 (14.5 [0–61])	Not applicable

ogy was assessed using the Scale for the Assessment of Positive Symptoms (SAPS) (Andreasen, 1984) and the Scale for the Assessment of Negative Symptoms (SANS) (Andreasen, 1983). Using the factor loadings reported by Andreasen and colleagues (Andreasen et al., 1995), we used the SAPS and SANS items to compute scores for three dimensions of psychopathology (*i.e.*, negative symptoms, psychosis and thought disorganization) in each of the individuals with schizophrenia.

2.2. Image collection

MR scans were collected on a Magnetom SP-4000 1.5-Tesla Siemens imaging system with a standard head coil using a turbo-FLASH sequence (TR=20 ms, TE=5.4 ms, flip angle=30°, 180 slices, 256-mm field of view, matrix=256×256, number of acquisitions=1, scanning time=13.5 min) that acquired three-dimensional datasets with 1 mm³ isotropic voxels across the entire cranium (Venkatesan and Haacke, 1997). MR datasets were reformatted using Analyze™ software (Analyze-AVW, 2004), and signed 16-bit MR datasets were compressed to unsigned 8-bit MR datasets by linearly rescaling voxel intensities such that voxels with intensity levels at two standard deviations above the mean of white matter (corpus callosum) were mapped to 255, and voxels with intensity levels at two standard deviations below the mean of CSF (lateral ventricle) were mapped to 0. The white matter and CSF means and standard deviations were obtained by sampling voxels from these respective regions. MR scans were then trilinearly interpolated into 0.5 mm³ isotropic resolution to produce smoother intensity histograms for more accurate segmentation. Prior to image processing, MR scans were coded and stripped of diagnostic group information. All subsequent processing including delineating cingulate gyrus surfaces (below) was performed on de-identified data. Clinical and demographic information was merged with imaging data in the statistical analysis step only after the cingulate gyrus measures were generated.

2.3. Anatomic definition of the cingulate gyrus

The medial limit of the cingulate gyrus was defined as the cortical surface within the interhemispheric fissure (Duvernoy, 1991). In coronal MR sections, the caudal end of the cingulate gyrus was defined by the isthmus, which lay below the splenium. The cingulate gyrus then followed the upper bank of the calcarine sulcus rostrally until the calcarine sulcus branched into the parietooccipital fissure. The cingulate gyrus was

separated from the precuneus by the subparietal sulcus where the cingulate sulcus turned upward to become the marginal sulcus. The superior limit of the cingulate gyrus was defined by the inferior bank of the cingulate sulcus. The inferior limit of the cingulate gyrus was formed by the superior bank of the callosal sulcus. Finally, the rostral end of the cingulate gyrus was defined as the most rostral coronal section through the septum pellucidum, the appearance of the paraolfactory sulcus being the delimiting landmark. The anterior segment of the cingulate gyrus (AC) was divided from the posterior segment (PC) of the structure using a plane passing through the anterior commissure (The plane passes through the anterior commissure at the point where it intersects the inter-hemisphere plane; this plane also is perpendicular to the line connecting the anterior and posterior commissures.). This border approximates the boundary between Brodmann areas (BA) 24 and 23 (Crosson et al., 1999; Heckers et al., 2004; Yucel et al., 2001).

The sulci and gyri within the AC may appear “doubled-up” in some individuals (Vogt et al., 1995). In some cases, the doubling-up consists of an intralimbic sulcus ventral to the cingulate sulcus; in other cases, the doubling-up consists of the paracingulate gyrus (PCG) dorsal to the cingulate sulcus (Paus et al., 1996; Yucel et al., 2001). According to Brodman, the PCG, when present, consists of a cortical region (BA 32) that is separable from the AC (Heckers et al., 2004; Paus et al., 1996). More specifically, BA 24 and 25 occupy the AC, while BA 32 is rostral and dorsal to BA 24b, dorsal to BA 24c and 24c', and terminates near BA 24c'g. BA 32 has a mixture of cytoarchitectural features of cingulate cortex and adjacent frontal and parietal cortical areas. Whenever PCG is absent, BA 32 is always limited to the dorsal bank of the cingulate sulcus (Heckers et al., 2004; Vogt et al., 1995). In the current study, 21 of the 53 individuals with schizophrenia had a left PCG and 10 had a right PCG; six individuals with schizophrenia had PCG in both hemispheres. Twenty-three of the 68 comparison subjects had a left PCG, and 17 had a right PCG; seven had PCG on both sides. There was no significant group difference in the frequency of PCG in either hemisphere: left $\chi^2=0.43$, $df=1$, $p=0.5$; right $\chi^2=0.65$, $df=1$, $p=0.42$.

2.4. Labeled cortical mantle distance mapping (LCMDM)

The development and implementation of LCMDM can be found in previous publications (Miller et al., 2003, 2000). In addition, the validation and application

of LCMDM to the analysis of the cingulate gyrus is described in detail in Ratnanather et al. (2004).

A region of interest (ROI) containing the entire cingulate gyrus was first manually defined in each pre-processed MR image (Fig. 1, panel a). Bayesian segmentation was then used to classify voxels within the ROI as cerebrospinal fluid (CSF), gray matter (GM), white matter (WM), partial CSF-GM (PCG), and partial GM-WM (PGW) by fitting the ROI histogram with five Gaussian curves representing each of the five tissue types (Joshi et al., 1999; Miller et al., 2000; Ratnanather et al., 2001) (Fig. 1, panel b). To define the GM/WM interface, the ROI was first binarized into WM at the optimal GM/WM threshold. The optimal threshold between GM and WM was determined based on the crossings between GM and PGW Gaussian curves and between PGW and WM Gaussian curves and a predetermined ratio (between 0 and 1). This ratio was obtained from a previously provided learning dataset of

expert manual segmentations of the cingulate gyrus in similar MR scans using Neyman–Pearson likelihood ratio test (Ratnanather et al., 2004). A topology correction method was then applied to the binary volume in which all handles of the WM object were removed. The original intensity of the modified voxels was adjusted to ensure that the binarization of the edited image was the same as the topologically correct binary image. An isosurface algorithm was then used to extract the isosurface from the edited image (Han et al., 2001, 2002) (Fig. 1, panel c, blue surface). Finally, dynamic programming was used to define the anatomic boundary of the cingulate subsurface on the GM/WM interface isosurface (Fig. 1, panel c, red surface). Anatomic boundaries were assumed to consist of a sequence of geodesics (the shortest path between two points on the isosurface) (Khaneja et al., 1998). The distance between each GM-labeled voxel in the segmented image and the subsurface was computed. This distance generated a

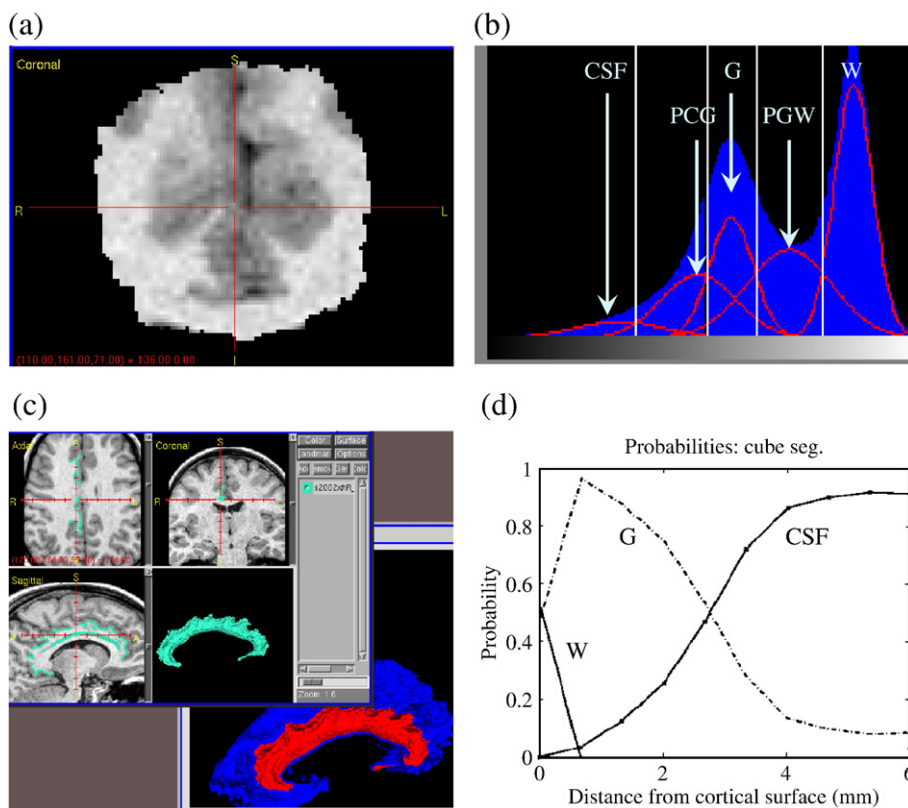


Fig. 1. Labeled Cortical Distance Mantle Mapping (LCMDM). (a) Region of interest (ROI): brain scan region containing the cingulate gyrus. (b) Mixture-of-Gaussians estimation in Bayesian tissue classification. (c) Delineated surface for the cingulate gyrus (red and teal) from the G/W interface isosurface (blue). (d) Probabilistic density functions for WM, GM and CSF. After integration to obtain cumulative distribution function, or CDF, GM thickness was calculated as the distance at the $p=0.9$ point (90th percentile) of the GM CDF. (For interpretation of the references to colour in this figure legend, the reader is referred to the web version of this article.)

histogram associated with GM labels (Miller et al., 2000; Ratnanather et al., 2001), which gave rise to probability and cumulative distribution functions (PDF, CDF) used in the analyses (Fig. 1, panel d, showing PDFs).

The inter-rater and intra-rater variabilities of delineating the cingulate gyrus subsurface were also examined, as previously described (Ratnanather et al., 2004). In ten randomly selected scans, two raters each delineated the cingulate gyrus surfaces. The surface areas had a mean absolute error of 0.077 with an intraclass correlation coefficient of 0.82. We randomly selected a scan to generate three slightly different regions of interest: the original ROI, and two additional ROIs by dilating the original ROI subvolume by $1 \times 1 \times 1$ and $3 \times 3 \times 3$ voxels. This produced three slightly different intensity histograms, which in turn produced three slightly different GM/WM boundary thresholds. As a result, we generated three surfaces from which one rater delineated all three cingulate gyrus surfaces. The coefficient of variation for the areas of the three surfaces was 0.043 and the pair-wise 90th-percentile distances between the three surfaces ranged from 0.14 to 0.21 mm.

2.5. Cingulate gyrus mantle measures

Trigonometry was used to calculate the surface area of the cingulate gyrus subsurface (Ratnanather et al., 2003, 2001). Gray matter volumes of the cingulate gyrus were calculated by integrating the GM distance histogram and then multiplying by the voxel dimensions. The 90th-percentile point of the CDF was used to represent the thickness of the cingulate gyrus gray matter mantle. The 90th-percentile point included 90% of the total cortical gray matter voxels encountered (*i.e.*, distance from the G/W interface surface). The CDF generated on the surface of the selected gyral surfaces was used to estimate the “mean thickness” across those subregions.

Total cerebral volumes were derived using Freesurfer (Desikan et al., 2006; Fischl et al., 2004) as the volume within the pial surface subtracting the volumes of the lateral ventricles and the ventral diencephalons. The structural measures of the cingulate gyrus were compared across groups using total cerebral volume as a covariate.

2.6. Statistical analyses

Because volume is a function of thickness and surface area (*i.e.*, in the simplest case, volume is the product of the latter two variables), we first performed a

primary group comparison of the volume of the two segments of the cingulate gyrus (*i.e.*, AC and PC) using one-way, repeated measures, mixed model ANOVA (SAS Institute Inc., 2000), with diagnosis as the between-individual factor and hemisphere as the repeated within-individual factor. Significance was reported for $\alpha=0.025$ (*i.e.* adjusting for multiple comparisons). Group differences in surface area, and thickness were then performed *post-hoc*, and significance was reported for one-tailed test of least squares means with unadjusted *p* values. Because of the variable presence of the PCG, all analyses of anterior cingulate measures were adjusted for the presence of the PCG. All ANOVA procedures were performed also with total cerebral brain volume as a covariate.

The relationships between the clinical variables and structural measures were examined in the individuals with schizophrenia using an exploratory correlation analysis. All correlations were estimated using non-parametric statistics (Spearman's rho) after partialing out total cerebral brain volume, and all correlations involving AC measures were done after partialing out the presence of the PCG. The significance of these correlations was reported after adjusting for multiple comparisons.

3. Results

The volume, surface area and thickness measures for the anterior and posterior segments of the left and right cingulate gyri are summarized in Table 2.

3.1. Cingulate gyrus volume

Individuals with schizophrenia had significantly smaller AC volumes than comparison subjects ($F=5.2$, $df=1118$, $p=0.024$). However, there was no significant effect of hemisphere ($F=1.8$, $df=1118$, $p=0.18$), nor was there a diagnosis-by-hemisphere interaction ($F=0.38$, $df=1118$, $p=0.54$). *Post-hoc* correlations between left and right AC volumes and total cerebral volumes were significant within the groups of individuals with schizophrenia (only right) and comparison subjects (see Table 3).

Individuals with schizophrenia also had significantly smaller PC volumes than comparison subjects ($F=14$, $df=1118$, $p=0.0005$). Again, there was no significant effect of hemisphere ($F=2.4$, $df=1119$, $p=0.13$), nor was there a significant diagnosis-by-hemisphere interaction ($F=0.20$, $df=1119$, $p=0.65$). *Post-hoc* correlations between the gray matter volumes of the PC and total cerebral volumes were significant within the

Table 2
Cingulate gyrus mantle measures: mean (SD) volume, surface area and thickness

		Schizophrenia		Comparison	
		L	R	L	R
Volume (cm ³)	AC *	37.7 (16.3)	40.1 (11.6)	44.8 (17.0)	43.10 (13.3)
	PC*	58.1 (11.0)	60.7 (11.4)	65.4 (11.1)	66.8 (11.4)
Surface area (cm ²)	AC	15.5 (6.2)	16.8 (5.5)	17.3 (6.4)	17.6 (5.7)
	PC	33.6 (7.4)	32.3 (7.5)	36.4 (6.4)	34.4 (6.0)
Thickness (mm)	AC*	2.38 (0.43)	2.10 (0.41)	2.44 (0.37)	2.13 (0.32)
	PC*	1.91 (0.34)	1.82 (0.34)	1.95 (0.26)	1.90 (0.29)
Total cerebral brain volume (cm ³)		952 (120)		1000 (108)	

* $p < 0.05$, schizophrenia versus controls, repeated measures ANOVA.

groups of individuals with schizophrenia and comparison subjects (see Table 3).

3.2. Cingulate gyrus thickness

Individuals with schizophrenia showed a trend toward significant difference in the thickness of the AC (schizophrenia < comparison subject: $t = 1.40$, $df = 118$, $p = 0.081$). Also, there was a significant effect of hemisphere ($F = 43$, $df = 1118$, $p < 0.0001$), but not a significant diagnosis-by-hemisphere interaction ($F = 0.06$, $df = 1118$, $p = 0.80$). *Post-hoc* correlations between the AC thickness and total cerebral volumes were not significant in either the group of schizophrenia or comparison subjects (see Table 3).

Individuals with schizophrenia also showed a trend toward significant difference in the thickness of the PC (schizophrenia < comparison subject: $t = 1.60$, $df = 118$, $p = 0.055$). There was no significant effect of hemisphere ($F = 3.5$, $df = 1119$, $p = 0.066$), nor a significant diagnosis-by-hemisphere interaction ($F = 0.27$, $df = 1119$, $p = 0.61$). *Post-hoc* correlations between the thickness of the PC and total cerebral volumes were not significant in either the group of schizophrenia or comparison subjects (see Table 3).

3.3. Cingulate gyrus surface area

The effect of diagnosis on the surface area of the AC was not significant (schizophrenia < comparison subject: $t = 1.00$, $df = 118$, $p = 0.16$). Also, there was no significant effect of hemisphere ($F = 0.05$, $df = 1118$, $p = 0.83$), nor was there a significant diagnosis-by-hemisphere interaction ($F = 0.04$, $df = 1118$, $p = 0.84$). *Post-hoc* correlations between the surface area of the AC and total cerebral volume were significant in the individuals with schizophrenia (right only) and comparison subjects (see Table 3).

The effect of diagnosis on the surface area of the PC also did not reach significance (schizophrenia < comparison subject: $t = 1.00$, $df = 118$, $p = 0.15$). There was a significant effect of hemisphere ($F = 4.3$, $df = 1119$, $p = 0.041$), but not a significant diagnosis-by-hemisphere interaction ($F = 0.17$, $df = 1119$, $p = 0.68$). *Post-hoc* correlations between the surface area of the PC and total cerebral volumes were significant in individuals with schizophrenia and comparison subjects (see Table 3).

Non-parametric correlations (Spearman's rho) among structural measures of the cingulate gyrus (volume, surface area and thickness) are summarized in Table 4.

Table 3
Correlations (Spearman's rho) between structural measures of the cingulate gyrus (volume, surface area and thickness) and total cerebral brain volume

Cingulate gyrus mantle measures ^a		Schizophrenia		Comparison	
		L	R	L	R
Volume	AC ^b	0.033 $p = 0.82$	0.29 $p = 0.045$	0.33 $p = 0.0072$	0.31 $p = 0.011$
	PC	0.20 $p = 0.12$	0.33 $p = 0.020$	0.50 $p < .0001$	0.49 $p < 0.001$
Surface area	AC ^b	0.20 $p = 0.17$	0.39 $p = 0.006$	0.37 $p = 0.0028$	0.25 $p = 0.047$
	PC	0.50 $p < .0001$	0.45 $p < .0001$	0.55 $p < .0001$	0.44 $p < .0001$
Thickness	AC ^b	-0.16 $p = 0.25$	-0.21 $p = 0.16$	-0.16 $p = 0.19$	-0.13 $p = 0.29$
	PC	-0.18 $p = 0.21$	-0.08 $p = 0.55$	-0.12 $p = 0.30$	0.024 $p = 0.85$

^a Significant ($p < 0.05$) correlations are shown in bold face.

^b Correlations with anterior measures were adjusted for presence of paracingulate gyrus.

Cingulate gyrus volume was generally correlated with both cingulate gyrus surface area and thickness.

3.4. Sex effect

When sex was included as a between-individual factor in the ANOVA analyses (in addition to diagnosis), a significant effect of sex was found for the volume of the AC ($m < f$, $p = 0.0003$), the thickness of the AC ($m < f$, $p < 0.0001$), the thickness of the PC ($m < f$, $p < 0.0001$), and for area of the PC ($m > f$, $p = 0.0005$). There was no gender by group interactions in any measures. Also, the diagnosis effect remained significant for the volume of the AC ($p = 0.05$) and PC ($p = 0.003$) after taking sex into account.

3.5. Relationships between neuroanatomical and clinical measures

Correlations between clinical features and structural measures were assessed in the individuals with schizophrenia in a *post-hoc*, exploratory analysis. There were trends toward inverse correlations between the duration of illness and the thickness of the left AC ($r = -0.29$, $p = 0.068$), right AC ($r = -0.29$, $p = 0.074$) and left PC ($r = -0.31$, $p = 0.054$). There were no other correlations between the structural measures and age of onset of illness or duration of illness.

Total SAPS scores were inversely correlated with the volume of the left AC ($r = -0.37$, $p = 0.033$). There were also trends toward inverse correlations between total SANS scores and volume of the left AC ($r = -0.29$, $p = 0.091$) and the thickness of the right AC ($r = -0.29$, $p = 0.088$). Also, the SAPS/SANS psychosis factor measure was inversely correlated with the volume of the left AC ($r = -0.39$, $p = 0.021$). The SAPS/SANS negative symptom factor measure also showed a trend toward an inverse correlation with the volume of the left AC ($r = -0.30$, $p = 0.089$). There were no other correlations between any other SAPS/SANS factor measures

and any structural measures of the PC. However, none of these correlations remained significant after correction of p values for multiple comparisons.

4. Discussion

The results of this study suggest that there is a reduction in the gray matter volume of the entire cingulate gyrus in individuals with schizophrenia; *i.e.*, this gray matter volume reduction is not confined to the anterior segment of the cingulate gyrus. The comparison of thickness and surface area measures in the individual groups suggest that this decrease in cingulate gyrus gray matter volume may be accounted for mostly by a decrease in the thickness of the cortical mantle. Interestingly, measures of illness severity, especially positive symptoms, and duration were associated with decreases in the gray matter volume of the AC, but not the PC. As expected, cingulate gyrus gray matter volume was highly correlated with both cingulate gyrus surface area and thickness, while surface area and thickness were only very weakly correlated.

The results of this study extend and perhaps help to resolve the contradictory results of prior *in vivo* neuroimaging studies of the cingulate gyrus in individuals with schizophrenia (Goldstein et al., 2002; Riffkin et al., 2005). Because of the variable convolutions of the cingulate gyrus, the precise delineation of the cingulate gyrus apart from neighboring cortical regions is challenging, and to the extent that this delineation is not precise, group differences can be obscured. Also, in many of the reported studies (Crespo-Facorro et al., 2000; Hirayasu et al., 1999; Mitelman et al., 2003, 2005; Narr et al., 2003; Sigmundsson et al., 2001), the description of the methods do not indicate whether the PCG was included or excluded in the measurement. If one were to include the PCG, this would result in the inclusion of BA 32, but only in those individuals with a PCG. Excluding the PCG eliminates this potential

Table 4

Correlations (Spearman's rho) among structural measures of the cingulate gyrus (volume, surface area and thickness), separately in each hemisphere and AC and PC

Cingulate measures ^a		L		R	
		Area	Thickness	Area	Thickness
AC ^b	Volume	0.82 ($p < .0001$)	0.36 ($p < .0001$)	0.73 ($p < .0001$)	0.22 ($p = 0.016$)
	Area	–	–0.057 ($p = 0.53$)	–	–0.39 ($p < .0001$)
PC	Volume	0.50 ($p < .0001$)	0.53 ($p < .0001$)	0.54 ($p < .0001$)	0.51 ($p < .0001$)
	Area	–	–0.33 ($p = 0.0003$)	–	–0.29 ($p = 0.0013$)

^a Correlations greater than 0.50 are shown in bold face.

^b Correlations of anterior measures were adjusted for presence of paracingulate gyrus.

confound. Moreover, because the retrosplenial (BA29 and BA30) cortex is consistently located on the ventral bank of the PC (BA 23 and 31) within the callosal sulcus, we included it as part of the PC. Even though the retrosplenial cortex and PC may subservise somewhat different functions, its inclusion with the PC in this study is supported by recent neuroanatomical studies of the two cortical regions (Mitelman et al., 2005; Vogt et al., 2005). Nonetheless, caution should be used in interpreting the results of any study of cortical structure where gross neuroanatomical landmarks, such as sulcal patterns, are used to delineate the boundaries of specific cortical regions, including our own. There is substantial normal variability in sulcal patterns and the relationship between such patterns and the true boundaries of specific cortical regions is not always consistent.

As mentioned above, cingulate gyrus gray matter volume loss in the individuals with schizophrenia appeared to be mostly accounted for by thinning of the cortical mantle, although a weaker trend toward a reduction in surface area was also observed. An illustration of the patterns of cortical thinning observed in the individual subjects with schizophrenia, and the distribution of cortical thickness values over the cingulate surface in a selection of schizophrenia and comparison subjects with extreme overall thickness values are shown in Figs. 2 and 3.

Although our analysis was exploratory, we found preliminary evidence for correlations between structural measures of the AC and clinical variables. In particular, reductions of surface area, gray matter volume and thickness in the left AC appeared to be related to the duration of illness as well as the severity of psychotic symptoms. An inverse correlation was also found between duration of illness and PC thickness. These preliminary findings suggest that there may be progressive changes in cingulate structure with increasing illness duration and that such changes may be related to worsening psychotic symptoms. Animal studies have shown that NMDA antagonists can selectively damage the PC (Olney and Farber, 1995). Also, increased NMDA receptor binding has been reported in the PC of schizophrenia patients, perhaps as the result of NMDA receptor hypofunction (Newell et al., 2005). Finally, decreased NAA/Cr ratios in the PC have been reported in patients with *chronic* schizophrenia that exhibit cognitive deficits (Shimizu et al., 2007). These findings, taken together with reports that NMDA receptor antagonists such as phencyclidine (PCP) and ketamine can cause schizophrenia-like psychosis and cognitive dysfunction in healthy humans (Andine et al., 1999; Javitt and Zukin, 1991; Malhotra et al., 1996) are

consistent with the more general hypothesis that NMDA receptor dysfunction could be the basis for neurodegenerative changes in the cingulate gyrus of patients with schizophrenia.

Since participants in this study had been treated with antipsychotic medications, it is unknown whether our correlational findings reflect relationships between neuroanatomical structure and the original severity of such symptoms or the degree to which antipsychotic medications affected them. Additional studies of individuals with schizophrenia who are untreated and in their first episode of illness or the family members of schizophrenia patients who are at increased risk for developing the disorder could be helpful in resolving such issues.

In this study, we used one of the new tools of computational anatomy (*i.e.*, Labeled Cortical Mantle Depth Mapping) to analyze the structural features of the cingulate gyrus. This method depends on the accuracy of both tissue classification and surface generation. Tissue misclassification rate is low — it usually occurs within one 0.5 mm^3 -voxel of the gray/white boundary. Surface generation is dependent on the accuracy of the threshold derived from the segmentation, and valid segmentation and surface reconstruction have been demonstrated in a variety of cortical regions including the cingulate gyrus (Miller et al., 2000; Ratnanather et al., 2003, 2001, 2004). Other potential sources of error are the definition of the anatomical boundaries of the cingulate proper (see above) and the possibility that some gray matter voxels are incorrectly incremented in the LCMDM histograms.

In sum, our results suggest that loss of gray matter, best represented by cortical mantle thinning, occurs across the entire contour of the cingulate gyrus in schizophrenia. However, measures of illness severity and duration appeared to be better correlated with thinning of the anterior segment of the cingulate gyrus. The cellular basis for thinning of the cortical mantle *versus* its surface area in disorders such as schizophrenia is unknown. However, we speculate that loss of pyramidal neurons or their processes would likely result in a reduction in both surface area and thickness, while the loss of nonpyramidal neurons (*i.e.*, interneurons) and their processes with a mainly vertical organization would likely result in a reduction of thickness alone. A recent meta-analysis of post-mortem studies of the cingulate gyrus in individuals with schizophrenia found that decreases in both pyramidal and non-pyramidal neurons and their processes is associated with schizophrenia (Todtenkopf et al., 2005) while the mechanism by which changes in neuronal architecture occurs in

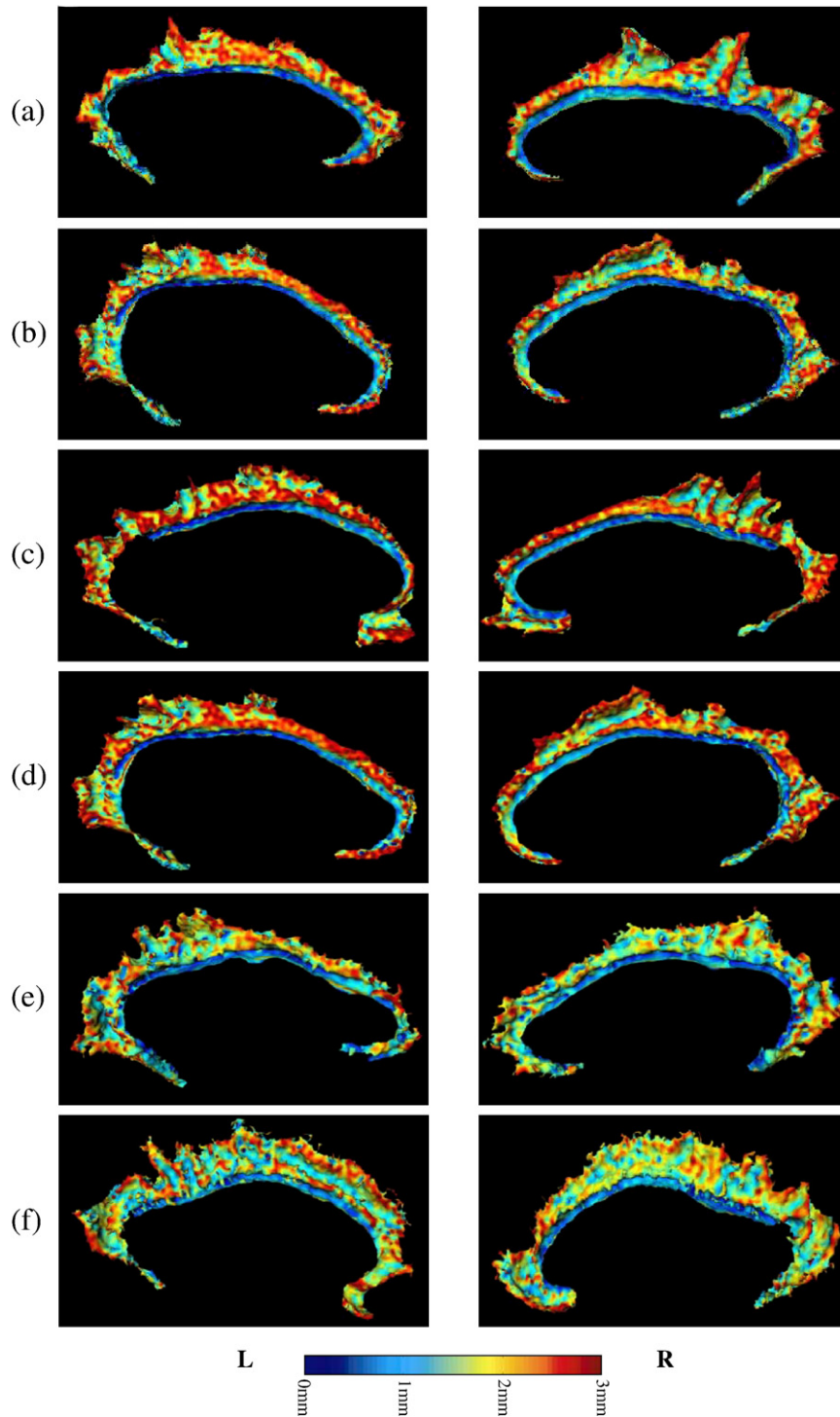


Fig. 2. Examples of cortical depth profile — comparison subjects. Examples of cortical gray matter thickness distribution (maps) over the cingulate surface as generated *via* LCMDM, in comparison subjects. Rows (a–c) show maps from three individuals with large thickness values in the right AC. Rows (d–f) show maps from three individuals with small thickness values in the right AC. For visualization, the maps have been smoothed *via* spline interpretations of the eigenfunctions of the Laplace–Beltrami operator (Qiu et al., 2005 (in revision)). (For interpretation of the references to colour in this figure legend, the reader is referred to the web version of this article.)

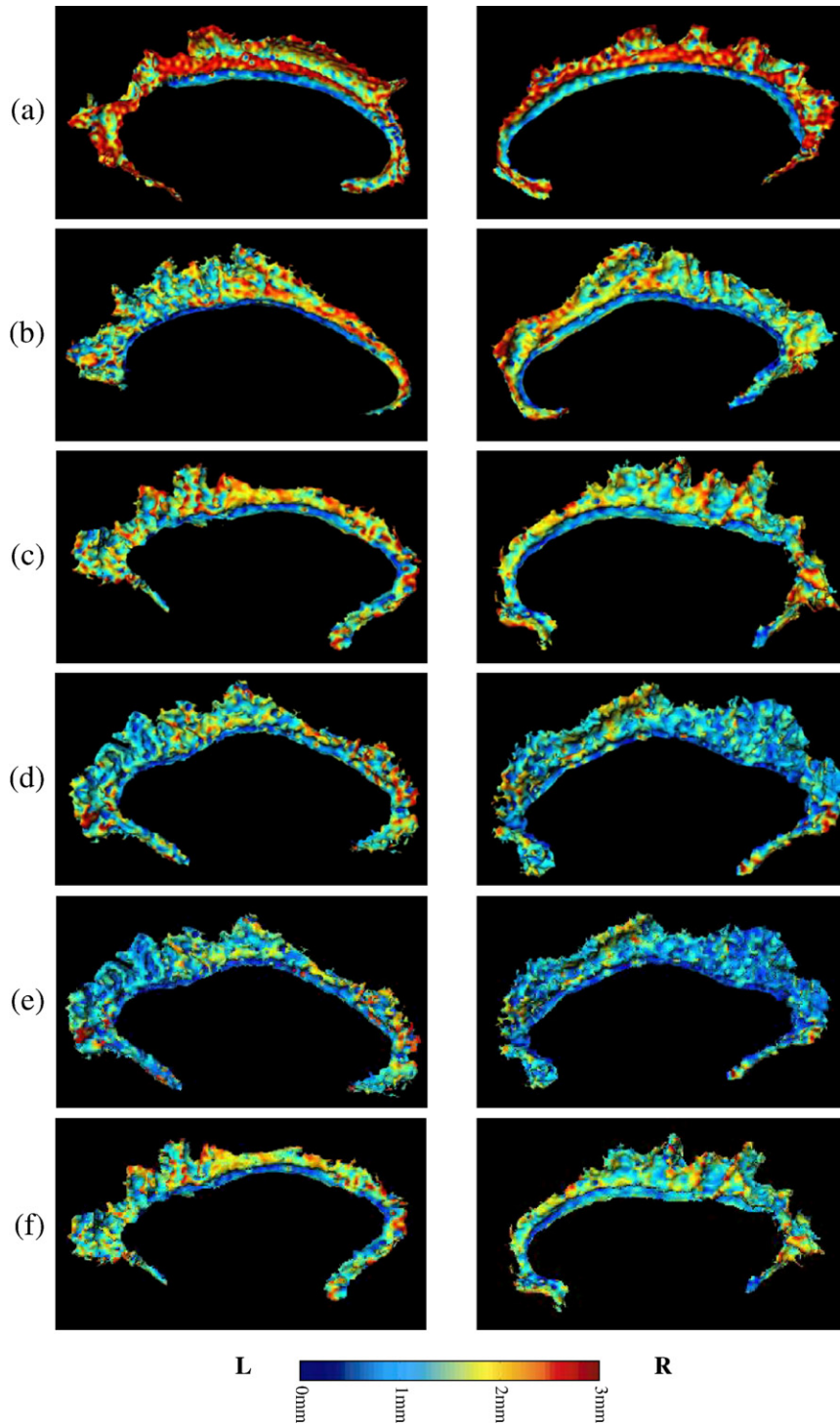


Fig. 3. Examples of cortical depth profile — schizophrenia individuals. Examples of cortical gray matter thickness distribution (maps) over the cingulate surface as generated *via* LCMDM, in schizophrenia individuals. Rows (a–c) show maps from three individuals with large thickness values in the right AC. Rows (d–f) show maps from three individuals with small thickness values in the right AC.

schizophrenia (*i.e.*, neurodevelopmental or neurodegenerative or both) remains unknown. NMDA receptor dysfunction has been implicated in both post-mortem studies of individuals with schizophrenia and animal models of disease pathogenesis.

Role of funding source

Funding for this study was provided by NIMH grants R01-MH056584, the Conte Center for the Neuroscience of Mental Disorders at Washington University School of Medicine (P20-MH071616) and P41-RR15241; the funding agencies had no further role in study design; in the collection, analysis and interpretation of data; in the writing of the report; and in the decision to submit the paper for publication.

Contributors

Study design: Lei Wang, J. Tilak Ratnanather, Mokhtar H. Gado, Michael I. Miller, and John G. Csernansky.

Data collection: Lei Wang, Malini Hosakere, Joshua C. L. Trein, and Alex Miller.

Analyses: Lei Wang and Anqi Qiu.

Statistical analysis: Lei Wang, Deanna M. Barch, and Paul A. Thompson.

Literature Search: Lei Wang, Mokhtar H. Gado, and John G. Csernansky.

Manuscript draft: Lei Wang and John G. Csernansky.

All authors contributed to and have approved the final manuscript.

References

- American Psychiatric Association, 1994. Diagnostic and statistical manual of mental disorders: DSM-IV, vol. xxvii. American Psychiatric Association, Washington, DC. 886 pp.
- Analyze-AVW, 2004. Analyze-AVW. Mayo Medical Foundation, Rochester, Minnesota.
- Andine, P., Widermark, N., Axelsson, R., Nyberg, G., Olofsson, U., Martensson, E., Sandberg, M., 1999. Characterization of MK-801-induced behavior as a putative rat model of psychosis. *J. Pharmacol. Exp. Ther.* 290, 1393–1408.
- Andreasen, N.C., 1983. The Scale for Assessment of Negative Symptoms (SANS). The University of Iowa, Iowa City, Iowa.
- Andreasen, N.C., 1984. The Scale for Assessment of Positive Symptoms (SAPS). The University of Iowa, Iowa City, Iowa.
- Andreasen, N.C., Swayze II, V.W., Flaum, M., Yates, W.R., Arndt, S., McChesney, C., 1990. Ventricular enlargement in schizophrenia evaluated with computed tomographic scanning. Effects of gender, age, and stage of illness. *Arch. Gen. Psychiatry* 47, 1008–1015.
- Andreasen, N.C., Arndt, S., Alliger, R., Miller, D., Flaum, M., 1995. Symptoms of schizophrenia. Methods, meanings, and mechanisms. *Arch. Gen. Psychiatry* 52, 341–351.
- Benes, F.M., 1991. Evidence for neurodevelopment disturbances in anterior cingulate cortex of post-mortem schizophrenic brain. *Schizophr. Res.* 5, 187–188.
- Benes, F.M., Bird, E.D., 1987. An analysis of the arrangement of neurons in the cingulate cortex of schizophrenic patients. *Arch. Gen. Psychiatry* 44, 608–616.
- Benes, F.M., McSparren, J., Bird, E.D., SanGiovanni, J.P., Vincent, S.L., 1991. Deficits in small interneurons in prefrontal and cingulate cortices of schizophrenic and schizoaffective patients. *Arch. Gen. Psychiatry* 48, 996–1001.
- Benes, F.M., Vincent, S.L., Todtenkopf, M., 2001. The density of pyramidal and nonpyramidal neurons in anterior cingulate cortex of schizophrenic and bipolar subjects. *Biol. Psychiatry* 50, 395–406.
- Bouras, C., Kovari, E., Hof, P.R., Riederer, B.M., Giannakopoulos, P., 2001. Anterior cingulate cortex pathology in schizophrenia and bipolar disorder. *Acta Neuropathol. (Berl)* 102, 373–379.
- Chana, G., Landau, S., Beasley, C., Everall, I.P., Cotter, D., 2003. Two-dimensional assessment of cytoarchitecture in the anterior cingulate cortex in major depressive disorder, bipolar disorder, and schizophrenia: evidence for decreased neuronal somal size and increased neuronal density. *Biol. Psychiatry* 53, 1086–1098.
- Cotter, D., Mackay, D., Landau, S., Kerwin, R., Everall, I., 2001. Reduced glial cell density and neuronal size in the anterior cingulate cortex in major depressive disorder. *Arch. Gen. Psychiatry* 58, 545–553.
- Crespo-Facorro, B., Kim, J., Andreasen, N.C., O’Leary, D.S., Magnotta, V., 2000. Regional frontal abnormalities in schizophrenia: a quantitative gray matter volume and cortical surface size study. *Biol. Psychiatry* 48, 110–119.
- Crosson, B., Sadek, J.R., Bobholz, J.A., Gokcay, D., Mohr, C.M., Leonard, C.M., Maron, L., Auerbach, E.J., Browd, S.R., Freeman, A.J., Briggs, R.W., 1999. Activity in the paracingulate and cingulate sulci during word generation: an fMRI study of functional anatomy. *Cereb. Cortex* 9, 307–316.
- Csernansky, J.G., Wang, L., Jones, D., Rastogi-Cruz, D., Posener, J.A., Heydebrand, G., Miller, J.P., Miller, M.I., 2002. Hippocampal deformities in schizophrenia characterized by high dimensional brain mapping. *Am. J. Psychiatry* 159, 2000–2006.
- Csernansky, J.G., Schindler, M.K., Splinter, N.R., Wang, L., Gado, M., Selemon, L.D., Rastogi-Cruz, D., Posener, J.A., Thompson, P.A., Miller, M.I., 2004a. Abnormalities of thalamic volume and shape in schizophrenia. *Am. J. Psychiatry* 161, 896–902.
- Csernansky, J.G., Wang, L., Joshi, S.C., Ratnanather, J.T., Miller, M.I., 2004b. Computational anatomy and neuropsychiatric disease: probabilistic assessment of variation and statistical inference of group difference, hemispheric asymmetry, and time-dependent change. *NeuroImage* 23 (Suppl 1), S56–S68.
- Desikan, R.S., Segonne, F., Fischl, B., Quinn, B.T., Dickerson, B.C., Blacker, D., Buckner, R.L., Dale, A.M., Maguire, R.P., Hyman, B.T., Albert, M.S., Killiany, R.J., 2006. An automated labeling system for subdividing the human cerebral cortex on MRI scans into gyral based regions of interest. *NeuroImage* 31, 968–980.
- Dolan, R.J., Fletcher, P., Frith, C.D., Friston, K.J., Frackowiak, R.S., Grasby, P.M., 1995. Dopaminergic modulation of impaired cognitive activation in the anterior cingulate cortex in schizophrenia. *Nature* 378, 180–182.
- Duvernoy, H.M., 1991. The Human Brain: Surface, Three-Dimensional Anatomy and MRI. Springer-Verlag, Wien, New York.
- First, M., Spitzer, R., Gibbon, M., Williams, J., 1995. Structured Clinical Interview for DSM-IV Axis I Disorders — Patient Edition

- (SCID-I/P, Version 2.0). Biometrics Research Department, New York State Psychiatric Institute, New York, NY.
- Fischl, B., Salat, D.H., Busa, E., Albert, M., Dieterich, M., Haselgrove, C., van der Kouwe, A., Killiany, R., Kennedy, D., Klaveness, S., Montillo, A., Makris, N., Rosen, B., Dale, A.M., 2002. Whole brain segmentation: automated labeling of neuroanatomical structures in the human brain. *Neuron* 33, 341–355.
- Fischl, B., Salat, D.H., van der Kouwe, A.J., Makris, N., Segonne, F., Quinn, B.T., Dale, A.M., 2004. Sequence-independent segmentation of magnetic resonance images. *NeuroImage* 23 (Suppl 1), S69–S84.
- Goldstein, J.M., Seidman, L.J., O'Brien, L.M., Horton, N.J., Kennedy, D.N., Makris, N., Caviness Jr., V.S., Faraone, S.V., Tsuang, M.T., 2002. Impact of normal sexual dimorphisms on sex differences in structural brain abnormalities in schizophrenia assessed by magnetic resonance imaging. *Arch. Gen. Psychiatry* 59, 154–164.
- Ha, T.H., Youn, T., Ha, K.S., Rho, K.S., Lee, J.M., Kim, I.Y., Kim, S.I., Kwon, J.S., 2004. Gray matter abnormalities in paranoid schizophrenia and their clinical correlations. *Psychiatry Res.* 132, 251–260.
- Han, X., Xu, C., Prince, J.L., 2001. A Topology Preserving Deformable Model Using Level Set, CVPR'2001. Kauai, HI, IEEE, pp. 765–770.
- Han, X., Xu, C.Y., Braga-Neto, U., Prince, J.L., 2002. Topology correction in brain cortex segmentation using a multiscale, graph-based algorithm. *IEEE Trans. Med. Imag.* 21, 109–121.
- Heckers, S., Weiss, A.P., Deckersbach, T., Goff, D.C., Morecraft, R.J., Bush, G., 2004. Anterior cingulate cortex activation during cognitive interference in schizophrenia. *Am. J. Psychiatry* 161, 707–715.
- Hirayasu, Y., Shenton, M.E., Salisbury, D.F., Kwon, J.S., Wible, C.G., Fischer, I.A., Yurgelun-Todd, D., Zarate, C., Kikinis, R., Jolesz, F.A., McCarley, R.W., 1999. Subgenual cingulate cortex volume in first-episode psychosis. *Am. J. Psychiatry* 156, 1091–1093.
- Hulshoff Pol, H.E., Schnack, H.G., Mandl, R.C., van Haren, N.E., Koning, H., Collins, D.L., Evans, A.C., Kahn, R.S., 2001. Focal gray matter density changes in schizophrenia. *Arch. Gen. Psychiatry* 58, 1118–1125.
- Javitt, D.C., Zukin, S.R., 1991. Recent advances in the phencyclidine model of schizophrenia. *Am. J. Psychiatry* 148, 1301–1308.
- Joshi, M., Cui, J., Doolittle, K., Joshi, S., Van Essen, D., Wang, L., Miller, M.I., 1999. Brain segmentation and the generation of cortical surfaces. *NeuroImage* 9, 461–476.
- Khaneja, N., Grenander, U., Miller, M.I., 1998. Dynamic Programming Generation of Curves on Brain Surfaces. *IEEE Trans. Pattern Anal. Mach. Intell.* 20, 1260–1264.
- Lawrie, S.M., Abukmeil, S.S., 1998. Brain abnormality in schizophrenia. A systematic and quantitative review of volumetric magnetic resonance imaging studies. *Br. J. Psychiatry* 172, 110–120.
- Malhotra, A.K., Pinals, D.A., Weingartner, H., Sirocco, K., Missar, C.D., Pickar, D., Breier, A., 1996. NMDA receptor function and human cognition: the effects of ketamine in healthy volunteers. *Neuropsychopharmacology* 14, 301–307.
- Miller, M.I., Massie, A.B., Ratnanather, J.T., Botteron, K.N., Csernansky, J.G., 2000. Bayesian construction of geometrically based cortical thickness metrics. *NeuroImage* 12, 676–687.
- Miller, M.I., Hosakere, M., Barker, A.R., Priebe, C.E., Lee, N., Ratnanather, J.T., Wang, L., Gado, M., Morris, J.C., Csernansky, J.G., 2003. Labeled cortical mantle distance maps of the cingulate quantify differences between dementia of the Alzheimer type and healthy aging. *Proc. Natl. Acad. Sci. U. S. A.* 100, 15172–15177.
- Mitelman, S.A., Shihabuddin, L., Brickman, A.M., Hazlett, E.A., Buchsbaum, M.S., 2003. MRI assessment of gray and white matter distribution in Brodmann's areas of the cortex in patients with schizophrenia with good and poor outcomes. *Am. J. Psychiatry* 160, 2154–2168.
- Mitelman, S.A., Shihabuddin, L., Brickman, A.M., Hazlett, E.A., Buchsbaum, M.S., 2005. Volume of the cingulate and outcome in schizophrenia. *Schizophr. Res.* 72, 91–108.
- Narr, K.L., Sharma, T., Woods, R.P., Thompson, P.M., Sowell, E.R., Rex, D., Kim, S., Asuncion, D., Jang, S., Mazziotta, J., Toga, A.W., 2003. Increases in regional subarachnoid CSF without apparent cortical gray matter deficits in schizophrenia: modulating effects of sex and age. *Am. J. Psychiatry* 160, 2169–2180.
- Narr, K.L., Toga, A.W., Szeszko, P., Thompson, P.M., Woods, R.P., Robinson, D., Sevy, S., Wang, Y., Schrock, K., Bilder, R.M., 2005. Cortical thinning in cingulate and occipital cortices in first episode schizophrenia. *Biol. Psychiatry* 58, 32–40.
- Newell, K.A., Zavitsanos, K., Huang, X.F., 2005. Ionotropic glutamate receptor binding in the posterior cingulate cortex in schizophrenia patients. *NeuroReport* 16, 1363–1367.
- Olney, J.W., Farber, N.B., 1995. Glutamate receptor dysfunction and schizophrenia. *Arch. Gen. Psychiatry* 52, 998–1007.
- Ongur, D., Drevets, W.C., Price, J.L., 1998. Glial reduction in the subgenual prefrontal cortex in mood disorders. *Proc. Natl. Acad. Sci. U. S. A.* 95, 13290–13295.
- Paus, T., Otaky, N., Caramanos, Z., MacDonald, D., Zijdenbos, A., D'Avirro, D., Gutmans, D., Holmes, C., Tomaiuolo, F., Evans, A.C., 1996. In vivo morphometry of the intrasulcal gray matter in the human cingulate, paracingulate, and superior-rostral sulci: hemispheric asymmetries, gender differences and probability maps. *J. Comp. Neurol.* 376, 664–673.
- Qiu, A., Bitouk, D., Miller, M.I., 2005. Smooth Functional and Structural Maps on the Neocortex via Orthogonal Bases of the Laplace–Beltrami Operator. *IEEE Trans. Med. Imag.* (in revision).
- Rastogi-Cruz, D., Csernansky, J., 1997. Clinical rating scales. In: Guze, S. (Ed.), *Adult Psychiatry*. Mosby, Inc., St. Louis.
- Ratnanather, J.T., Botteron, K.N., Nishino, T., Massie, A.B., Lal, R.M., Patel, S.G., Peddi, S., Todd, R.D., Miller, M.I., 2001. Validating cortical surface analysis of medial prefrontal cortex. *NeuroImage* 14, 1058–1069.
- Ratnanather, J.T., Barta, P.E., Honeycutt, N.A., Lee, N., Morris, H.M., Dziorny, A.C., Hurdal, M.K., Pearlson, G.D., Miller, M.I., 2003. Dynamic programming generation of boundaries of local coordinated submanifolds in the neocortex: application to the planum temporale. *NeuroImage* 20, 359–377.
- Ratnanather, J.T., Wang, L., Nebel, M.B., Hosakere, M., Han, X., Csernansky, J.G., Miller, M.I., 2004. Validation of semiautomated methods for quantifying cingulate cortical metrics in schizophrenia. *Psychiatry Res.* 132, 53–68.
- Riffkin, J., Yucel, M., Maruff, P., Wood, S.J., Soulsby, B., Olver, J., Kyrios, M., Velakoulis, D., Pantelis, C., 2005. A manual and automated MRI study of anterior cingulate and orbito-frontal cortices, and caudate nucleus in obsessive-compulsive disorder: comparison with healthy controls and patients with schizophrenia. *Psychiatry Res.* 138, 99–113.
- SAS Institute Inc., 2000. SAS System for Windows, V8. SAS Institute Inc., Cary, North Carolina.
- Shimizu, E., Hashimoto, K., Ochi, S., Fukami, G., Fujisaki, M., Koike, K., Okamura, N., Ohgake, S., Koizumi, H., Matsuzawa, D., Zhang, L., Watanabe, H., Nakazato, M., Shinoda, N., Komatsu, N., Morita, F., Iyo, M., 2007. Posterior cingulate gyrus metabolic changes in chronic schizophrenia with generalized cognitive deficits. *J. Psychiatr. Res.* 41, 49–56.
- Sigmundsson, T., Suckling, J., Maier, M., Williams, S., Bullmore, E., Greenwood, K., Fukuda, R., Ron, M., Toone, B., 2001. Structural

- abnormalities in frontal, temporal, and limbic regions and interconnecting white matter tracts in schizophrenic patients with prominent negative symptoms. *Am. J. Psychiatry* 158, 234–243.
- Todtenkopf, M.S., Vincent, S.L., Benes, F.M., 2005. A cross-study meta-analysis and three-dimensional comparison of cell counting in the anterior cingulate cortex of schizophrenic and bipolar brain. *Schizophr. Res.* 73, 79–89.
- Uematsu, M., Kaiya, H., 1989. Midsagittal cortical pathomorphology of schizophrenia: a magnetic resonance imaging study. *Psychiatry Res.* 30, 11–20.
- Van Leemput, K., Maes, F., Vandermeulen, D., Suetens, P., 2003. A unifying framework for partial volume segmentation of brain MR images. *IEEE Trans. Med. Imag.* 22, 105–119.
- Venkatesan, R., Haacke, E., 1997. Role of high resolution in magnetic resonance (MR) imaging: applications for MR angiography, intracranial T1-weighted imaging, and image interpolation. *Int. J. Imaging Syst. Technol.* 8, 529–543.
- Vogt, B.A., Nimchinsky, E.A., Vogt, L.J., Hof, P.R., 1995. Human cingulate cortex: surface features, flat maps, and cytoarchitecture. *J. Comp. Neurol.* 359, 490–506.
- Vogt, B.A., Vogt, L., Laureys, S., 2005. Cytology and functionally correlated circuits of human posterior cingulate areas. *NeuroImage*.
- Wright, I.C., Rabe-Hesketh, S., Woodruff, P.W., David, A.S., Murray, R.M., Bullmore, E.T., 2000. Meta-analysis of regional brain volumes in schizophrenia. *Am. J. Psychiatry* 157, 16–25.
- Young, A.H., Blackwood, D.H., Roxborough, H., McQueen, J.K., Martin, M.J., Kean, D., 1991. A magnetic resonance imaging study of schizophrenia: brain structure and clinical symptoms. *Br. J. Psychiatry* 158, 158–164.
- Yucel, M., Stuart, G.W., Maruff, P., Velakoulis, D., Crowe, S.F., Savage, G., Pantelis, C., 2001. Hemispheric and gender-related differences in the gross morphology of the anterior cingulate/paracingulate cortex in normal volunteers: an MRI morphometric study. *Cereb. Cortex* 11, 17–25.
- Yucel, M., Stuart, G.W., Maruff, P., Wood, S.J., Savage, G.R., Smith, D.J., Crowe, S.F., Copolov, D.L., Velakoulis, D., Pantelis, C., 2002. Paracingulate morphologic differences in males with established schizophrenia: a magnetic resonance imaging morphometric study. *Biol. Psychiatry* 52, 15–23.